IMPULSIVE LOADING OF CELLULAR MEDIA IN SANDWICH CONSTRUCTION

Joseph A. Main[1] **and George A. Gazonas**[2]

[1]*Building and Fire Research Laboratory, National Institute of Standards and Technology*
100 Bureau Drive, Mail Stop 8611, Gaithersburg, MD 20899-8611
[2]*Weapons and Materials Research Directorate, U.S. Army Research Laboratory*
ATTN: AMSRD-ARL-WM-MD, Aberdeen Proving Ground, MD 21005-5069

Abstract. Motivated by recent efforts to mitigate blast loading using energy-absorbing materials, this paper investigates the uniaxial crushing of cellular media in sandwich construction under impulsive pressure loading. The cellular core is modeled using a rigid, perfectly-plastic, locking idealization, as in previous studies, and the front and back faces are modeled as rigid, with pressure loading applied to the front face and the back face unrestrained. Predictions of this analytical model show excellent agreement with explicit finite element computations, and the model is used to investigate the influence of the mass distribution between the core and the faces. Increasing the mass fraction in the front face is found to increase the impulse required for complete crushing of the cellular core but also to produce undesirable increases in back-face accelerations. Optimal mass distributions are investigated by maximizing the impulse capacity while limiting the back-face accelerations to a specified level.

Keywords: Blast mitigation, aluminum foam, shock wave, finite element analysis.
PACS: 46.40.Cd, 62.50.+p, 83.60.Uv.

BACKGROUND

Cellular materials such as metal foams and honeycombs are being considered in a wide variety of structural applications because of their capacity to absorb impact energy. Surprisingly, however, their use under blast loading has often led to enhancement, rather than mitigation, of blast effects. Experiments by Hanssen et al. [1] showed that increased upswing results from the addition of an aluminum foam layer to the face of a massive "pendulum" subjected to blast loading. Nesterenko [2] noted that in these experiments, the blast impulse is imparted primarily to a lightweight plate covering the foam layer, leading to significantly higher kinetic energy than if the same impulse were imparted directly to the more massive pendulum. Xue and Hutchinson [3] noted a similar effect in a computational study of blast loading on sandwich plates, in which the kinetic energy imparted to a sandwich plate was observed to be greater than for a solid plate of the same mass. In spite of this, it was found that deflections of sandwich plates could be significantly less than for the corresponding solid plate. Xue and Hutchinson considered front and back face sheets with equal mass but suggested that further reductions in deflections might be achieved by increasing the mass fraction in the face sheet near the blast.

ANALYTICAL MODEL

Motivated by these observations, an analytical model is developed in this paper to investigate the influence of mass distribution on the uniaxial crushing of cellular material sandwiched between rigid layers. The cellular core material is represented by the simplified stress-strain relationship shown in Fig. 1(b), originally proposed by Reid and Peng [4] for modeling crushing of wood and subsequently applied to cellular metals in a number of studies (e.g., [1,5]). Arbitrary masses of the front and back faces are permitted, and a pressure pulse $p(t)$ is applied to the front face with the back face unrestrained. This sandwich model is a generalization of that in [1], which considered a fixed back face, and of that in [5], which considered front and back faces of equal mass with blast loading represented by an initial velocity imparted to the front face.

A strip of sandwich panel with unit cross-sectional area is considered, with total mass given by $m = m_1 + \rho_0 \ell_0 + m_2$, where ρ_0 and ℓ_0 are the uncompressed density and thickness of the cellular core, and m_1 and m_2 are the areal densities of the front and back faces. The acceleration of the center of mass, denoted $\ddot{u}_G$, follows directly from application of Newton's second law to the strip:

$$p(t) = m\ddot{u}_G \tag{1}$$

Provided the applied pressure is sufficiently high, densification of the cellular core commences at the front face, and a densification front propagates through the core. By conservation of mass, the density of the compressed core material is $\rho_0/(1-\varepsilon_0)$. According to the simplified model of Fig. 1(b), the compressed core material moves as a rigid body with the same velocity as the front face, denoted $\dot{u}_1$, while the uncompressed core material moves as a rigid body with the velocity of the back face, $\dot{u}_2$. The stress just ahead of the densification front is σ_0, and application of Newton's second law to the material ahead of the densification front then yields the following equation:

$$\sigma_0 = (\rho_0 x + m_2)\ddot{u}_2 \tag{2}$$

where x denotes the thickness of the uncompressed core material, and the thickness of the densification front itself is assumed to be negligible. By forming and differentiating an expression for x_G, the distance of the center of mass from the back face, it follows that

$$\ddot{x}_G = (\varepsilon_0/m)\left\{\left[m_1 + \rho_0(\ell_0 - x)\right]\ddot{x} - \rho_0\dot{x}^2\right\} \tag{3}$$

Eqs. (1) - (3) can then be combined through the relation $\ddot{u}_2 = \ddot{u}_G + \ddot{x}_G$ to yield the following nonlinear ordinary differential equation for x:

$$\begin{aligned} -\varepsilon_0\left[m_1 + \rho_0(\ell_0 - x)\right]\ddot{x} + \varepsilon_0\rho_0\dot{x}^2 \\ = p(t) - \sigma_0 m/(\rho_0 x + m_2) \end{aligned} \tag{4}$$

Eq. (4) can be integrated numerically with initial conditions $x(0) = \ell_0$ and $\dot{x}(0) = 0$. A triangular pressure pulse is considered, as shown in Fig. 1(c), with total impulse denoted i_∞. The following symbols are introduced to denote the nondimensional peak pressure and total impulse:

$$P_0 = \frac{p_0}{\sigma_0}; \; I_\infty = \frac{i_\infty}{m}\sqrt{\frac{\rho_0}{\sigma_0\varepsilon_0}} \tag{5}$$

The following symbols denote the mass fractions in the core and in the front and back faces:

$$\eta_0 = \rho_0\ell_0/m; \; \eta_1 = m_1/m; \; \eta_2 = m_2/m \tag{6}$$

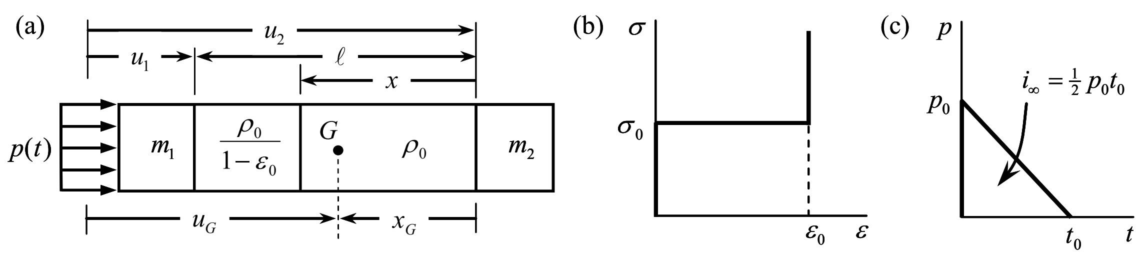

Figure 1. Analytical model definition: (a) Strip of sandwich panel with partially compacted core; (b) Stress vs. volumetric strain relationship for core material; (c) Triangular pressure pulse applied to front face.

Table 1. Parameters of computational simulations.

Case	η_1	η_0	η_2	P_0	I_∞
pendulum	0.0125	0.0125	0.975	10	0.015
sandwich	0.25	0.5	0.25	10	1

COMPARISON WITH COMPUTATIONS

The predictions of the analytical model are compared with explicit finite element computations using LS-DYNA. In the computations, the cellular core was represented by a single row of solid elements with total thickness ℓ_0 = 5 cm, using material model 26 (*MAT_HONEYCOMB) with ρ_0 = 250 kg/m^3, σ_0 = 1 MPa, and ε_0 = 0.7. A large elastic modulus of E = 700 GPa was used to represent the "rigid" portions of the idealized stress-strain relationship in Fig. 1(b), and Poisson's ratio was set to zero. The material viscosity coefficient μ was set to 0.001, and 150 elements were found to be sufficient for convergence.

The front and back faces were represented in the computations by added nodal masses, and two different mass distributions were considered, as indicated in Table 1. The "pendulum" case corresponds to the blast pendulum experiments of [1], with the large back-face mass representing the pendulum. The "sandwich" case corresponds to the sandwich plates of [3] and [5], with equal front-face and back-face masses.

In Figs. 2 and 3, computational results are compared with predictions of the analytical model, and good agreement is observed. Results are plotted against nondimensional time, $\tau = (\sigma_0 / i_\infty)t$. The nondimensional velocities in Figs. 2 and 3 are defined as $\bar{v}_1 = \dot{u}_1 / v_\infty$ and $\bar{v}_2 = \dot{u}_2 / v_\infty$, where $v_\infty = i_\infty / m$ is the final velocity of the center of mass. Due to the small mass of the front face, much larger nondimensional front-face velocities are observed in the "pendulum" case, despite the much smaller nondimensional impulse I_∞ in this case, as shown in Table 1.

INFLUENCE OF MASS DISTRIBUTION

Fig. 3(a) shows contours of the critical nondimensional impulse I_∞ for which complete densification of the core is first achieved. These contours correspond to the limiting case of a Dirac delta impulse ($P_0 \to \infty$) and were obtained by numerical solution of Eq. (4). Fig. 3(a) shows that increasing the mass fraction in the core and in the front face increases the impulse capacity of the sandwich system. However, Fig. 3(b) shows that increasing the mass fraction in the core and in the front face also leads to increased back-face accelerations, thus sacrificing a protective function of the cellular core. The nondimensional back-face accelerations presented in Fig. 3(b) are defined as $\bar{a}_2 = (m/\sigma_0)\ddot{u}_2$. It follows from Eq. (2) that the peak back-face accelerations occur at the instant of complete compaction (x = 0), for which $\ddot{u}_2 = \sigma_0 / m_2$ or $\bar{a}_2 = 1/\eta_2$. A design optimization problem can be posed by seeking to maximize the impulse I_∞ that can be sustained while limiting the back-face accelerations to a specified level. Fig. 4 shows a contour plot of the maximum impulse I_∞ that can be sustained with accelerations limited to $\bar{a}_2 = 5$. The grey curve in Fig. 4 corresponds to $1/\eta_2 = 5$. Below this curve, the values of

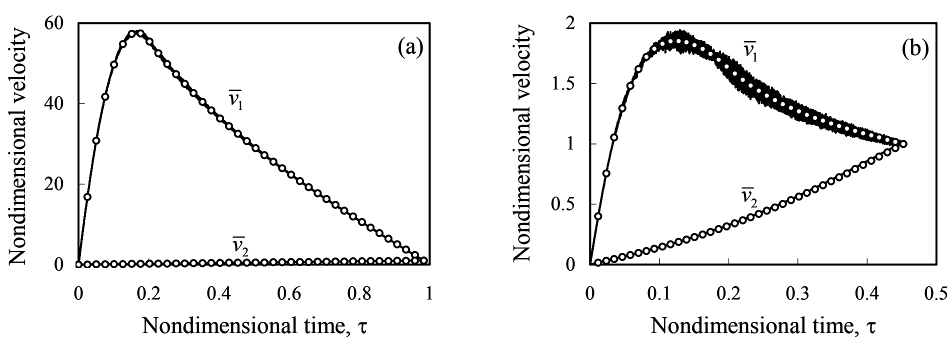

Figure 2. Comparison of LS-DYNA computations (—) with predictions of analytical model (○): Nondimensional front-face and back-face velocities for (a) "pendulum" case; (b) "sandwich" case.

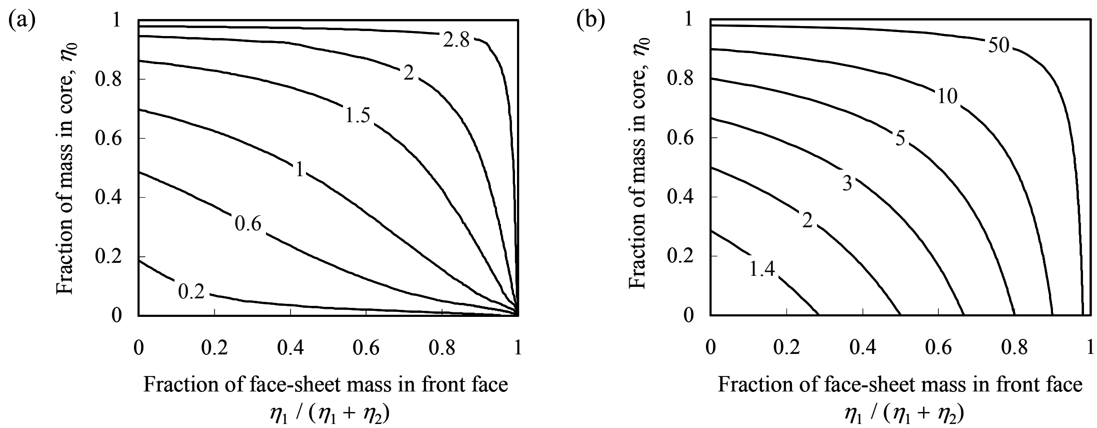

Figure 3. Contours with varying mass distribution: (a) Critical nondimensional impulse I_∞ required for complete compaction of core ($P_0 \to \infty$); (b) Peak nondimensional back-face acceleration $\bar{a}_2$ at complete compaction of core.

maximum impulse correspond to complete compaction of the core and are the same as in Fig. 3(a). Above this curve, $\bar{a}_2 > 5$ at complete compaction, so only partial compaction is permitted and the values of maximum impulse are less than in Fig. 3(a). In the shaded region of Fig. 4, defined by $(\eta_0 + \eta_2)^{-1} > 5$, $\bar{a}_2 > 5$ at initiation of compaction, so the maximum allowable impulse is zero. It is evident in Fig. 4 that for a given mass fraction in the core η_0, the allowable impulse is maximized along the grey curve, i.e., by adjusting the mass distribution so that the acceleration at complete compaction equals the allowable value.

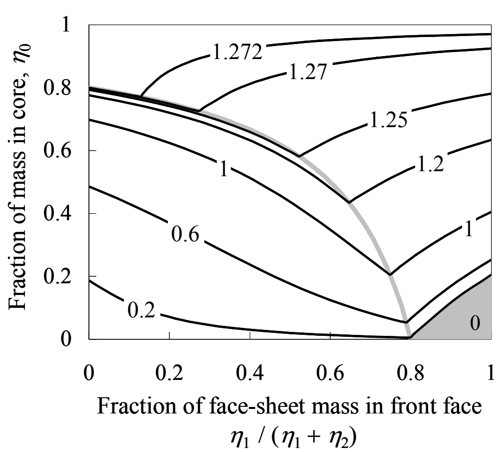

Figure 4. Contours of maximum nondimensional impulse I_∞ with nondimensional back-face accelerations limited to $\bar{a}_2 = 5$.

ACKNOWLEDGEMENTS

This work was supported in part by an appointment of the first author to the Postgraduate Research Participation Program at the U.S. Army Research Laboratory (ARL) administered by the Oak Ridge Institute for Science and Education through an interagency agreement between the Department of Energy and ARL.

REFERENCES

1. Hanssen, A. G., Enstock, L., and Langseth, M. "Close-range blast loading of aluminum foam panels." *Int. J. Impact Eng.* **27**, 593-618 (2002).
2. Nesterenko, V. F. "Shock (blast) mitigation by 'soft' condensed matter." *MRS Proceedings*, Vol. 759 (2002).
3. Xue, Z. and Hutchinson, J. W. "Preliminary assessment of sandwich plates subject to blast loads." *Int. J. Mech. Sci.* **45**, 687-705 (2003).
4. Reid, S. R. and Peng, C. "Dynamic uniaxial crushing of wood." *Int. J. Impact Eng.* **19**, 531-570 (1997).
5. Fleck, N. A. and Deshpande, V. S. "The resistance of clamped sandwich beams to shock loading." *J. Appl. Mech.* **71**, 386-401 (2004).